Journal of Magnetic Resonance 203 (2010) 66–72

Contents lists available at ScienceDirect

Journal of Magnetic Resonance

journal homepage: www.elsevier.com/locate/jmr

Field strength dependence of PRESS timings for simultaneous detection of glutamate and glutamine from 1.5 to 7 T

Jeff Snyder [a,b,*], Alan Wilman [a,c]

[a] Department of Physics, University of Alberta, Edmonton, Alta., Canada
[b] Medical Physics, Department of Diagnostic Radiology, University Hospital Freiburg, Freiburg, Germany
[c] Department of Biomedical Engineering, University of Alberta, Edmonton, Alta., Canada

ARTICLE INFO

Article history:
Received 24 July 2009
Revised 1 December 2009
Available online 4 December 2009

Keywords:
Glutamate
Glutamine
Magnetic resonance spectroscopy
Spectral editing
PRESS
Strong coupling
PRESS timings
High field MRS

ABSTRACT

An optimization of the PRESS sequence for magnetic resonance spectroscopy is presented to simultaneously detect the important brain metabolites of glutamate (Glu) and glutamine (Gln) at field strengths of 1.5, 3, 4.7, and 7 T. Standard, clinical examinations typically use short echo times which in general are not ideal for the separation of Glu and Gln. The optimization procedure is based on numerical product operator simulations to produce yield and overlap measurements for all possible practical choices of PRESS inter-echo timings. The simulations illustrate the substantial modulations in Glu and Gln with field strength. At all field strengths, the optimized timings demonstrate a significant reduction in overlap compared to short echo PRESS, while maintaining a high metabolite signal, with Glu and Gln yields >90% when excluding T2 relaxation losses. Minimal overlap was attained at 7 T (0.3% Gln contamination in the Glu signal), and 4.7 T (1.2%). The optimized timings were applied in vivo on healthy volunteers at field strengths of 1.5 and 4.7 T.

1. Introduction

Proton nuclear magnetic resonance spectroscopy (MRS) is a valuable tool to investigate the metabolic properties of the human brain non-invasively. Most metabolites in the human brain are coupled spin systems, and display a degree of spectral complexity, with phase and multiplet height dependent on timing parameters. These coupled spin systems have a narrow chemical shift range leading to significant resonance overlap at clinical magnetic field strengths. A particularly difficult quantification problem is that of the separation of glutamate (Glu) and glutamine (Gln). The similar chemical compositions of Glu, an important neurotransmitter, and its inactive form, Gln, result in similar resonance frequencies and spectral patterns, producing a large overlapping region at standard, short echo timings and clinical field strengths. This overlap tends to decrease the accuracy of the chosen fitting method, with a corresponding decrease in concentration accuracy [1].

Many spectral editing methods have been proposed to aid in quantification of coupled spin systems, and Glu and Gln specifically, such as multiple quantum filtering and tailored pulses [2–6], subtraction spectroscopy [7–9], *J*-resolved methods [10], and 2D spectroscopy [11,12]. With the exception of very simple difference spectroscopy methods, these editing techniques require specialized pulse sequences deviating from the standard PRESS and STEAM, which may not be available on all clinical systems. In addition, multiple quantum filtering in general does not provide a complete spectrum due to the editing process and difference spectroscopy requires rigorous post-processing schemes to correct for frequency drifts and is susceptible to dynamic spectrometer errors which may reduce the accuracy of the subtraction. The simplest editing technique involves manipulating the timing parameters of the particular spectroscopy sequence (TE1, TE2 – PRESS; TE_S, TM – STEAM) to produce different *J*-coupling evolutions and reduce spectral complexity and/or overlap for the target metabolite. No spectral information is lost and this method can be used with standard sequences and processing schemes. In terms of the Glu/Gln resonances, this method has been explored to a limited extent at multiple field strengths using the STEAM sequence [13,14], and at 3 T using the PRESS sequence [15–17].

In this study, we explore the optimization of timing parameters using a standard PRESS sequence in an effort to eliminate spectral overlap between Glu and Gln at field strengths of 1.5, 3, 4.7 and 7 T. The emphasis of the study is the choice of asymmetric PRESS timings in order to detect Glu and Gln simultaneously. The parameters were investigated first using theory and spin simulations, with supporting in vivo experiments at 1.5 and 4.7 T.

* Corresponding author. Address: University Hospital Freiburg, Department of Diagnostic Radiology, Medical Physics, Hugstetterstr. 55, 79106 Freiburg, Germany. Fax: +49 761 270 9379.
E-mail address: jeff.snyder@uniklinik-freiburg.de (J. Snyder).

1090-7807/$ - see front matter © 2009 Elsevier Inc. All rights reserved.
doi:10.1016/j.jmr.2009.12.002

2. Methods

Glu and Gln are both strongly coupled five-spin systems and can be characterized as AMNPQ using the Pople notation [18], with the PQ resonance (protons attached to the fourth carbon) typically being the target for quantification in vivo. The central resonance frequencies for the PQ group are in the range of 2.33–2.35 ppm for Glu, and 2.43–2.45 ppm for Gln, with *J*-couplings of −15.92 and −15.37 Hz for Glu and Gln [19], respectively. The MN peaks, originating from protons attached to the 3rd carbon of Glu and Gln (with resonance frequencies occurring in the range 2.03–2.13 ppm) are predominantly obscured by the strong NAA singlet resonance originating at 2.01 ppm, and the comparable resonant frequencies of the A peaks (second carbon protons with frequencies of ∼3.75 ppm) strongly hinders Glu/Gln discrimination.

The optimization method focuses on the PQ resonances and takes into account two main parameters: yield of the PQ peaks (area and height) and total overlap of Glu and Gln. In addition, the reduction of the outer peaks of the PQ systems was investigated similar to the method proposed by Trabesinger [20]. A selection of spectra produced by the most favourably predicted TE points were inspected visually prior to decision on the 'best' optimized timings.

2.1. Numerical simulations

Numerical simulations were performed to determine the response of Glu and Gln to a standard PRESS sequence ($90^\circ - \frac{TE1}{2} - 180^\circ - \frac{TE1}{2} - \frac{TE2}{2} - 180^\circ - \frac{TE2}{2} -$ ACQ, TE1 = first echo time, TE2 = second echo time), using an in-house spin simulation program [16] (other programs are available [21]) that incorporates chemical shifts, coupling constants, and strong coupling effects for each metabolite. The numerical simulation program has been verified experimentally with results shown previously in [2,16,22–27]. The program segments the sequence into individual, time-independent Hamiltonians characterized as a radiofrequency (RF) pulse, gradient, or time delay. Following each segment in the sequence, the density matrix was calculated and used as the starting point in subsequent segments, with the production of a half echo (sampled transverse magnetization following TE) as the endpoint. In the case of amplitude modulated soft pulses, the pulse was further divided into small pieces, each encompassing a small time period relative to the full pulse, and each having an individual Hamiltonian. The small time period of each piece allowed the use of time-independent Hamiltonians, and the effects of chemical shift and *J*-coupling were included in each pulse piece. The complete evolution of the density matrix due to the soft pulses was achieved by summation of the effects over each piece.

The simulations were conducted for all practical values in TE space. TE space is defined as a rectangular grid, with coordinates of TE1 and TE2 corresponding to the Cartesian coordinates of y and x, respectively. The total echo time of the PRESS experiment, TE, is therefore a combination of these two coordinates (TE = TE1 + TE2). The included values of TE1 and TE2 were contained in the range of 10–205 ms. For each time point, spectra for Glu, Gln and Glx (Glu + Gln) were produced, with the Glx spectrum comprised of a 3:1 Glu:Gln physiological concentration ratio [28,29]. TE space area and peak height maps were produced for the PQ resonances of Glu and Gln to determine the regions of maximum signal yield. At short TE, each PQ resonance is composed of a multiplet with decreasing peak amplitude from its center. In an effort to minimize the overlap, peak height and area maps were also produced for each detectable peak in the PQ multiplet to investigate possible reductions in the amplitude of adjacent Glu and Gln outer wings – essentially collapsing the multiplet into a singlet [14]. At each time point in TE space, the contributions of Glu and Gln to the total Glx signal were calculated in the 2.0–2.6 ppm range, as well as the total amount of overlap in set regions determined by the frequencies of the collapsed Glu and Gln and short-echo spectra. Based on these criteria of yield and overlap, the optimal time point was chosen. As a final validation, a select number of spectra in the range of the optimized timings were inspected visually. The entire process was repeated for field strengths of 1.5, 3, 4.7 and 7 T. Short echo time spectra were also calculated for Glu and Gln (symmetric PRESS, TE1 = TE2 = 15 ms) to compare to the optimized results, and demonstrate the metabolite overlap at the four field strengths.

2.2. In vivo experiments

Single voxel spectroscopy experiments were performed on healthy volunteers giving informed consent using the optimized PRESS timings chosen from the simulation at 1.5 and 4.7 T. A $2 \times 2 \times 2$ cm^3 voxel was placed in parietal grey matter to maximize the Glu concentration [28], with the power calibrated to produce maximum signal from the water peak for the voxel. Other sequence parameters included 256 averages, and a repetition time of 1500 ms, resulting in a total acquisition time of 6 min, 24 s.

The 4.7 T experiments were performed using a Varian INOVA whole body MRI system, equipped with a 4 kW RF amplifier, a maximum gradient strength of 35 mT/m and maximum slew rate of 117 T/m∗s. A quadrature, 16-element birdcage head coil was used for transmission and reception. A Siemens Sonata equipped with a 15 kW RF amplifier, 40 mT/m gradient set and slew rate of 200 T/m∗s was used for the 1.5 T experiments. The 1.5 T system used a body coil for transmission and a single head coil for reception.

3. Results

3.1. Parameter optimization

Fig. 1 displays the Glu and Gln short echo time (TE = 30 ms) symmetric PRESS simulation spectra for the four different field strengths. The structure of the PQ multiplet is not readily realized at 1.5 T due to the obstructing MN resonances. However, at higher field strengths (3 T and greater), it is apparent that each PQ resonance has three main peaks at the chosen broadened linewidth of 3 Hz. The high degree of overlap between the MN and PQ groups at 1.5 T also prohibits the separate resolution of Glu and Gln at a short echo time of 30 ms. Discrimination between Glu and Gln in the 3 and 4.7 T spectra may be possible, as both Glu and Gln multiplets include non-overlapping peaks in the PQ region (2.3–2.6 ppm). At 4.7 T, the PQ peaks suffer only minimal overlap. In Fig. 1d, the same spectra are shown for a field strength of 7 T, illustrating the near complete resolution of the Glu/Gln PQ multiplets. It should be noted that the linewidths used in the simulations may not be obtainable in vivo and the spectra are for comparison only.

Illustrations of the lineshapes of the PQ Glu and Gln multiplets at different points in TE space are shown in Fig. 2 for 3 (a) and 4.7 T (b). For Glu, the central peak retains a positive height with varying amplitude for almost all of TE space (see also Fig. 3b and c) while the two outer peaks fluctuate between negative and positive values. The three peaks in the Gln multiplet all fluctuate between positive and negative heights. It should be noted that the appearance of the spectra return to the approximate shape of the short echo case in the range of TE = 110 ms to TE = 140 ms. This agrees in general with the $2\pi/\Lambda$ periodicity for a strongly coupled spin system shown in [20], with the strong coupling frequency, Λ, defined as:

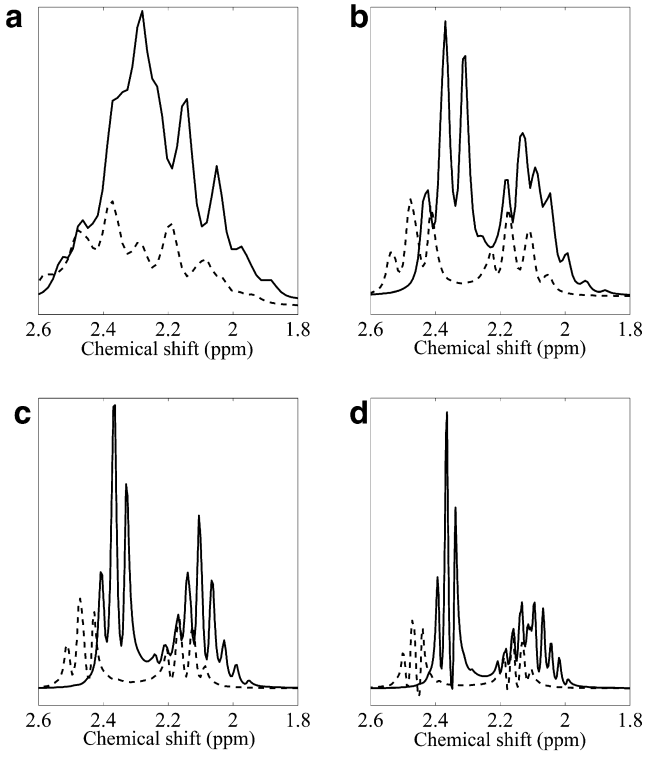

Fig. 1. Simulated short echo time (TE = 30 ms) symmetric PRESS spectra of Glu (solid line) and Gln (dashed) at field strengths of (a) 1.5 T, (b) 3 T, (c) 4.7 T, and (d) 7 T. All spectra were line broadened to 3 Hz. Relaxation effects are not included. The spectra are not to scale.

$$\Lambda = \sqrt{(\pi\Delta\nu)^2 + (\pi J)^2}, \quad (1)$$

where $\Delta\nu$ is the chemical shift difference (Hz) and J is the coupling constant (Hz) for the PQ group. A complete analytical description of the height variation for all peaks in the Glu and Gln PQ multiplet, also investigated based on the method in [20], is not possible based solely on a strongly coupled two spin approximation due to the dependency of PQ peak modulations on the entire AMNPQ system. However, it is evident in the numerical approach shown that spectra from several TE space time points show favourable lineshapes allowing the possible separate detection of Glu and Gln.

Fig. 3 shows the yield of Glu as a TE space map of the central PQ peak height. The values are normalized to the short echo PRESS case (TE1 = TE2 = 10 ms). At all field strengths, the greatest peak heights (besides the short echo case) are found approximately on the TE = 110 ms diagonal line. This is also apparent in the spectra shown in Fig. 2. Consequently, the best yield should occur roughly near TE = 110 ms, and is used in subsequent spectral overlap reduction experiments as an initial condition. Similar maps were produced for Gln (not shown) with maximum yield occurring at similar TEs as Glu.

The lineshape analysis and TE space simulation maps provided an initial starting point for Glu and Gln detection in the PQ region (2.3–2.6 ppm). At each field strength, the extent (range in frequency) of Glu and Gln was determined from the short TE spectra and select longer TE spectra, generally those conforming to simplified lineshapes (*i.e.* along the constant TE line of ~110 ms shown in Fig. 2). A main intersection point between Glu and Gln was defined, yielding two specific regions: (1) a Glu dominant region with Gln contaminants, and (2) a Gln dominant region with Glu contamination. For each of the half echoes (1600) acquired from the simulations, the contribution of Glu in region 1 and Gln in region 2 was calculated as an area fraction of the total signal per region (Glx). To obtain a value reflecting the amount of overlap in the two regions, the fractions were averaged. These values were then plotted in modified TE space maps, displaying an estimation of the total overlap between Glu and Gln (Fig. 4). A value approaching 1 in the maps denotes complete resolution (no overlap).

At 1.5 T (Fig. 4a), only a small region in TE space provides a significant reduction in the amount of overlap, and occurs approximately along parts of the constant TE line (diagonal in the TE map) of 110 ms, about 20 ms less than $2\pi/\Lambda$ (Glu – 126 ms; Gln – 130 ms). A similar trend is also seen for the maps at other field strengths, with increasing reduction in overlap with higher field, and a slight tendency to a reduction in the constant TE line value, roughly mirroring the decrease of the strong coupling period ($2\pi/\Lambda$) with increasing field. At 7 T (Fig. 4d) many points in TE space offer substantial resolution of the PQ groups. At moderate high fields of 4.7 T and especially 3 T, a wide range of overlap values is possible, and therefore careful choice of TE1 and TE2 is essential to Glu/Gln resolution.

In total, the data presented in Figs. 2–4 were used to determine the best timings. A small number of spectra which appeared optimal from both the overlap and peak height TE maps were inspected visually and the final optimized time points were chosen to obtain the least possible Glu/Gln overlap while maintaining large yield and relatively simple lineshapes of the PQ peaks.

The simulated Glu and Gln spectra at the optimal timings determined are shown in Fig. 5a–d for 1.5, 3, 4.7 and 7 T, respectively. Each plot contains the Glu (dashed line) and Gln (dotted) spectrum,

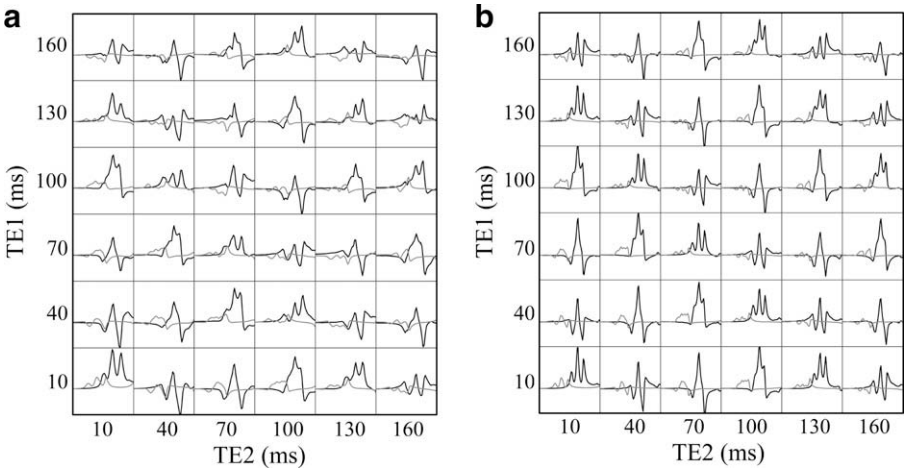

Fig. 2. Simulated spectra at different combinations of TE1 and TE2 for (a) 3 T and (b) 4.7 T. The chemical shift range for each spectrum is 2.25–2.55 ppm to focus on the PQ multiplets of Glu (black) and Gln (grey). All spectra have been line broadened using a 3 Hz exponential filter.

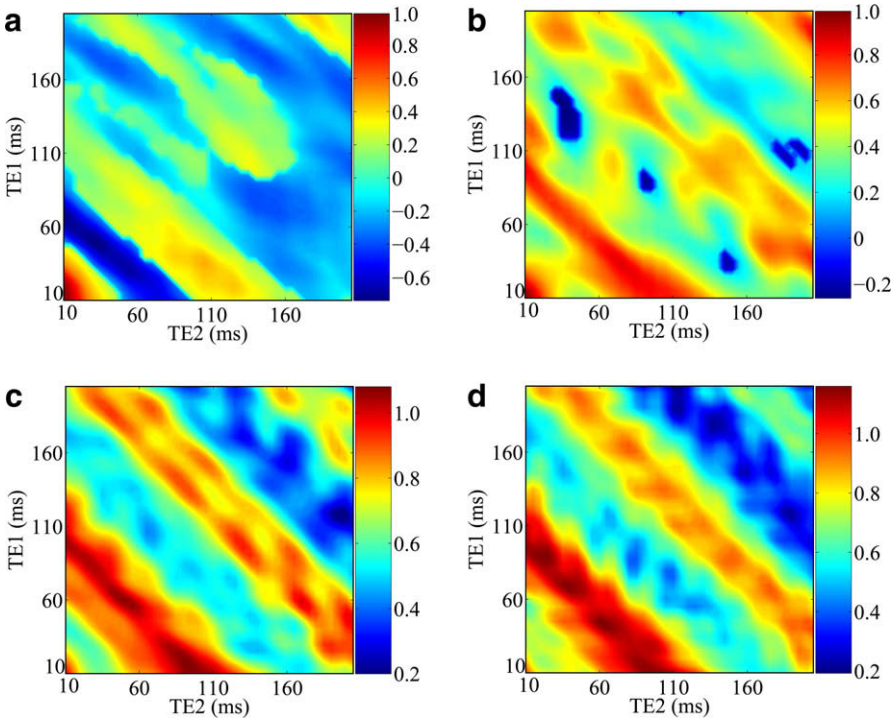

Fig. 3. Intensity maps of the central peak height of the Glu PQ multiplet in TE space at field strengths of (a) 1.5 T, (b) 3 T, (c) 4.7 T, and (d) 7 T. The yields are presented as a fraction of that obtained for a short (TE1 = TE2 = 10 ms) PRESS experiment.

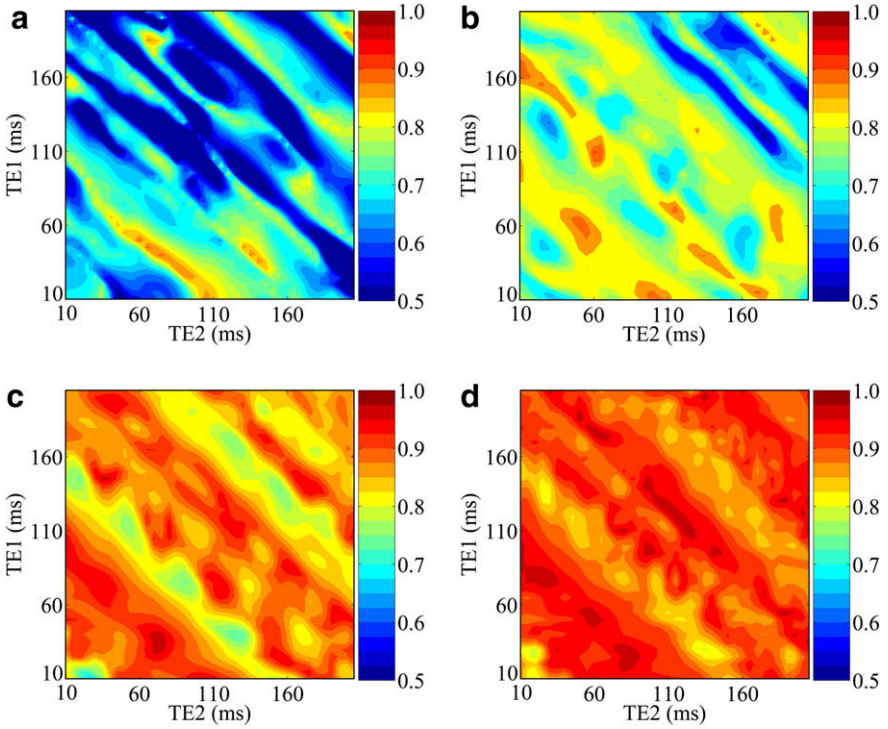

Fig. 4. TE space maps reflecting the fraction of overlap of the Glu and Gln PQ multiplets. The intensity is normalized such that a value of 1 indicates no overlap, while 0 is complete overlap. The maps correspond to field strengths of 1.5, 3, 4.7 and 7 T shown in (a)–(d), respectively.

and the resultant Glx (solid). The shaded regions correspond to the PQ regions calculated from the simulation to be predominantly Glu (right box, region 1) and Gln (left box, region 2). The signal composition was then recalculated in these two regions to determine the extent of Glu/Gln discrimination. Table 1 shows the percentage yield for each metabolite comprising the total Glx signal in each of the highlighted regions.

In Fig. 5a, the optimal timings for the PRESS experiment were calculated to be TE1 = TE2 = 55 ms for 1.5 T. Considering the appearance of the short TE spectra in Fig. 1a, the optimization of the

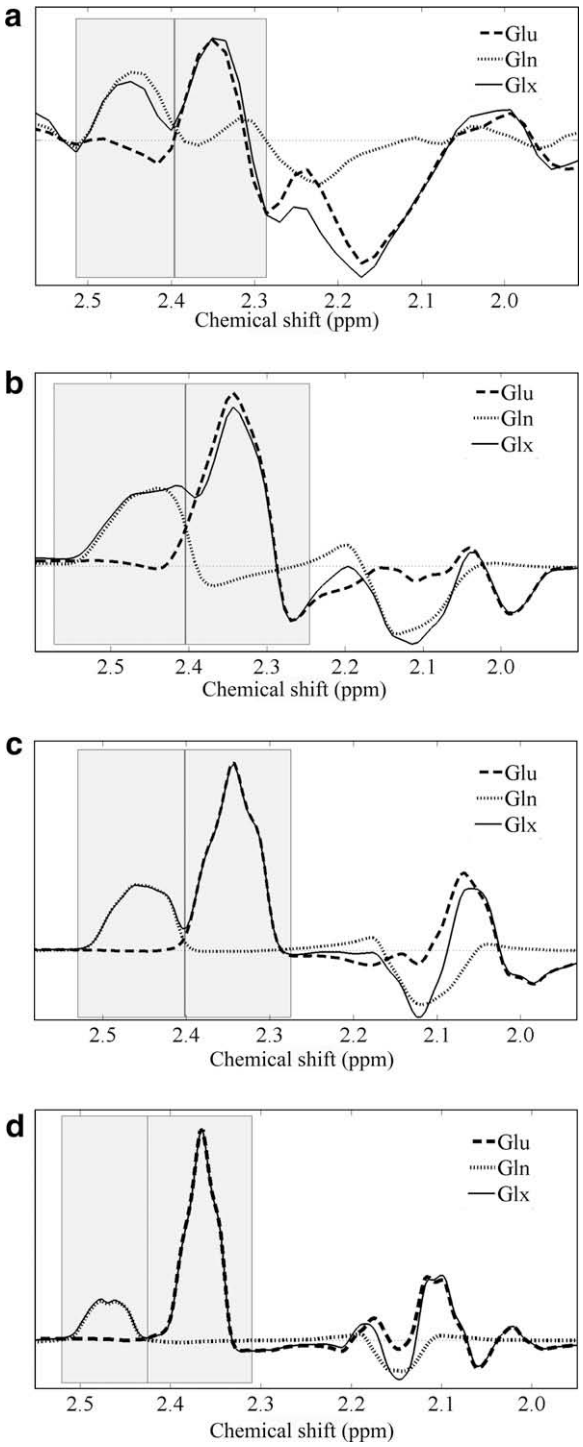

Fig. 5. Simulated spectra at optimized timings for Glu (dashed line), Gln (dotted line) and the resultant Glx (solid line) for (a) 1.5 T, (b) 3 T, (c) 4.7 T and (d) 7 T. The shaded region denotes the area where the overlap between Glu and Gln is computed, with Glu and Gln PQ ranges determined prior to the calculation.

timing parameters have offered a drastic improvement in resolution. Gln has the most contamination from Glu at this field strength, with 31% of the total signal composed of Glu in the Gln region. The intersection at 2.4 ppm of Glu and Gln almost extends to the baseline, and may improve the accuracy of a fitting routine. At 3 T (Fig. 5b), the timings as determined from the simulation were TE1 = 30 ms, and TE2 = 85 ms. These simulations show an improvement in signal composition in the two regions, although the intersection of the Glu and Gln lines is not as sharp as at 1.5 T. The overlap has virtually been eliminated at 4.7 T, with Glu and Gln percent compositions of 98.8 and 95.8 in their respective regions. The timings for the 4.7 T simulations were determined to be TE1 = 20 ms and TE2 = 90 ms. At 7 T, the optimized timings were TE1 = 20 ms and TE2 = 85 ms. Although a minor decrease in overlap can be noted for the results at 7 T, it is not a significant change compared to that from 3 to 4.7 T. The intersection of the collapsed multiplets appears near the baseline at 4.7 T (Fig. 3c) and the increase in field strength to 7 T merely shifts the Glu and Gln peaks further apart, which may be beneficial at broader linewidths. The results indicate that the best reduction in signal overlap should occur at 7 T, with minimal contamination; however, nearly identical results are apparent at 4.7 T.

Table 1
Metabolite area composition for Glu and Gln at 1.5, 3, 4.7 and 7 T[a].

Region	1.5 T		3 T		4.7 T		7 T	
	Glu	Gln	Glu	Gln	Glu	Gln	Glu	Gln
Glu (1)	83.5	16.5	89.6	10.4	98.8	1.2	99.7	0.3
Gln (2)	31.0	69.0	22.0	78.0	4.2	95.8	4.1	95.9

[a] Values presented are expressed as a percent of the total Glx area.

The calculated peak height yields for Glu and Gln at the optimized timings are given in Table 2. Both Glu and Gln show increasing yield with field strength. Results of the peak height measurement for 1.5 T may also include some contribution from the MN resonances. The yields are expressed as a percentage of the peak height obtained for the short echo symmetric PRESS case of TE = 20 ms.

3.2. In vivo experiments

The in vivo data are shown in Fig. 6 for (a) 1.5 T and (b) 4.7 T using the optimized timing parameters. The theoretical line shapes for Gln and Glu are also shown below the acquired spectra. The resolution shown for the simulated spectra in Fig. 6a is not apparent in the in vivo spectra, due to the large linewidth at 1.5 T, leading to a significant overlap (grey box in 6a), and therefore the expected possibility of discrimination is not realized. The increased resolution in the 4.7 T experiment allows the overlap to be minimized similar to the simulations. The theoretical lineshapes agree with the in vivo spectrum, and therefore cross-contamination between the two is expected to be minimal as predicted.

4. Discussion

The main value of this work was the demonstration that optimized timings could be generated at all field strengths from 1.5 to 7 T to provide significant improvement in signal yield and overlap minimization compared to short echo time spectra for the detection of Glu and Gln in the PQ range (2.3–2.6 ppm). This work may be used to determine best PRESS timings, but also to illustrate the significant field strength dependencies of these strongly coupled systems, which include dependencies on total echo time, PRESS asymmetry and multiplet shape. The timings were chosen to minimize the intensity of the outer peaks of each PQ multiplet, effectively reducing the contamination of Glu in the Gln region and vice versa. The complexity of the Glu and Gln AMNPQ systems prevented a direct, analytical approach to reducing the outer peaks of

Table 2
Calculated peak heights (yield) of Glu and Gln at optimized timings as a percentage of the short echo time PRESS signal (TE1 = TE2 = 10 ms) at 1.5, 3, 4.7 and 7 T.

	1.5 T	3 T	4.7 T	7 T
Glu	28.2	83.7	107.9	113.6
Gln	40.0	90.0	92.0	93.6

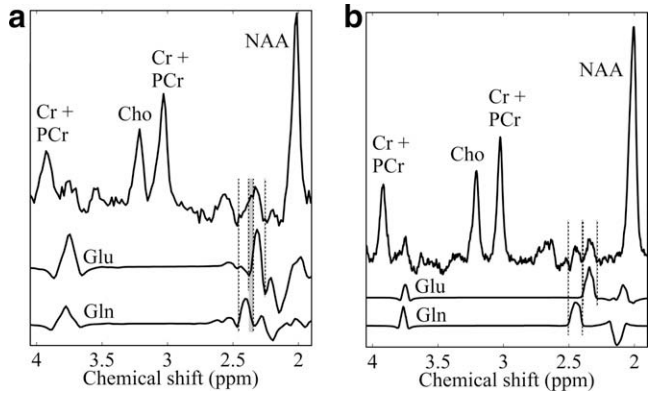

Fig. 6. In vivo spectra acquired at optimized timings determined from the simulation at a field strength of (a) 1.5 T (TE1 = TE2 = 55 ms), and (b) 4.7 T (TE1 = 20 ms, TE2 = 90 ms). The simulated spectra for Glu and Gln are shown below. The overlap of the two simulations is shown as a grey box in (a). Other sequence parameters included a voxel size of 8 cm^3, TR = 1500 ms, and 256 averages.

the PQ multiplet, instead full numerical simulations were necessary.

As expected, the overlap was the least at 7 T, with only a 0.3% and 4.1% cross-contamination for Glu and Gln, respectively. However, the results at 4.7 T were similar, with only a greater separation between the PQ peaks appearing at 7 T. The results at 4.7 T showed good lineshape agreement between numerical simulations and experiment. The optimized timings also provide less spectral overlap than those at standard, clinical short echo times (Fig. 1), even at triple the linewidth (9 Hz). At 1.5 and 3 T, distinction between Glu and Gln becomes more difficult, although Glu can be visualized at 3 T with only 10% contamination (Table 1). Previous work on PRESS optimization at 3 T [15] illustrated good Glu SNR, with a large uncertainty in the Gln concentration. At 1.5 T, discrimination is more difficult; however, the distinct intersection of Glu and Gln (Fig. 5a) may prove useful if experimental line broadening can be reduced further through improved shimming.

In addition to the reduction in spectral overlap, the quantification of Glu and Gln also requires accounting for macromolecular contamination [30], which has been shown to decrease the reliability of reported concentrations [31]. Other metabolites may also overlap Glu and Gln at the optimized timings, particularly γ-aminobutyric acid (GABA) with Glu (2.28 ppm) and aspartyl resonances with Gln (2.5–2.65 ppm). A similar investigation including all overlapping metabolites in the Glu/Gln range could be performed to increase the in vivo applicability. The simultaneous detection of Glu, Gln and GABA was previously reported for a STEAM sequence at 4 T [13]. Also, the effects of field strength on the Glu/Gln yields with the STEAM sequence have been investigated [14]. While the STEAM sequence can produce good results, it will generally have a reduced SNR when compared to PRESS.

In conclusion, this work has illustrated the significant modulation of Glu and Gln with field strength, and the need for careful choice of timing parameters to ensure minimal overlap and high yield in PRESS spectroscopy.

Acknowledgment

We are grateful for operating support from the National Science and Engineering Research Council of Canada (NSERC).

References

[1] R. Bartha, D.J. Drost, P.C. Williamson, Factors affecting the quantification of short echo in vivo 1H MR spectra: prior knowledge, peak elimination, and filtering, NMR Biomed. 12 (4) (1999) 205–216.

[2] R.B. Thompson, P.S. Allen, A new multiple quantum filter design procedure for use on strongly coupled spin systems found in vivo: its application to glutamate, Magn. Reson. Med. 39 (5) (1998) 762–771.

[3] A.H. Wilman, P.S. Allen, Yield enhancement of a double-quantum filter sequence designed for the edited detection of GABA, J. Magn. Reson. B 109 (2) (1995) 169–174.

[4] A. Yahya, B. Madler, B.G. Fallone, Exploiting the chemical shift displacement effect in the detection of glutamate and glutamine (Glx) with PRESS, J. Magn. Reson. 191 (1) (2008) 120–127.

[5] C. Choi, N.J. Coupland, P.P. Bhardwaj, N. Malykhin, D. Gheorghiu, P.S. Allen, Measurement of brain glutamate and glutamine by spectrally-selective refocusing at 3 tesla, Magn. Reson. Med. 55 (5) (2006) 997–1005.

[6] C.H. Choi, N.J. Coupland, P.P. Bhardwaj, S. Kalra, C.A. Casault, K. Reid, P.S. Allen, T-2 measurement and quantification of glutamate in human brain in vivo, Magn. Reson. Med. 56 (5) (2006) 971–977.

[7] D.L. Rothman, K.L. Behar, H.P. Hetherington, R.G. Shulman, Homonuclear 1H double resonance difference spectroscopy of the rat brain in vivo, Proc. Natl. Acad. Sci. USA 81 (20) (1984) 6330–6334.

[8] G. Gambarota, M. van der Graaf, D. Klomp, R.V. Mulkern, A. Heerschap, Echo-time independent signal modulations using PRESS sequences: a new approach to spectral editing of strongly coupled AB spin systems, J. Magn. Reson. 177 (2) (2005) 299–306.

[9] J. Snyder, R.B. Thompson, A.H. Wilman, Difference spectroscopy using PRESS asymmetry: application to glutamate, glutamine, and myo-inositol, NMR Biomed. (2009), doi:10.1002/nbm.1424.

[10] H.K. Lee, A. Yaman, O. Nalcioglu, Homonuclear J-refocused spectral editing technique for quantification of glutamine and glutamate by 1H NMR spectroscopy, Magn. Reson. Med. 34 (2) (1995) 253–259.

[11] H. Watanabe, N. Takaya, F. Mitsumori, Simultaneous observation of glutamate, gamma-aminobutyric acid, and glutamine in human brain at 4.7 T using localized two-dimensional constant-time correlation spectroscopy, NMR Biomed. 21 (5) (2008) 518–526.

[12] R. Hurd, N. Sailasuta, R. Srinivasan, D.B. Vigneron, D. Pelletier, S.J. Nelson, Measurement of brain glutamate using TE-averaged PRESS at 3T, Magn. Reson. Med. 51 (3) (2004) 435–440.

[13] J.N. Hu, S.L. Yang, Y. Xuan, Q. Jiang, Y.H. Yang, E.M. Haacke, Simultaneous detection of resolved glutamate, glutamine, and gamma-aminobutyric acid at 4 T, J. Magn. Reson. 185 (2) (2007) 204–213.

[14] S.L. Yang, J.N. Hu, Z.F. Kou, Y.H. Yang, Spectral simplification for resolved glutamate and glutamine measurement using a standard STEAM sequence with optimized timing parameters at 3, 4, 4.7, 7, and 9.4 T, Magn. Reson. Med. 59 (2) (2008) 236–244.

[15] F. Schubert, J. Gallinat, F. Seifert, H. Rinneberg, Glutamate concentrations in human brain using single voxel proton magnetic resonance spectroscopy at 3 Tesla, Neuroimage 21 (4) (2004) 1762–1771.

[16] R.B. Thompson, P.S. Allen, Sources of variability in the response of coupled spins to the PRESS sequence and their potential impact on metabolite quantification, Magn. Reson. Med. 41 (6) (1999) 1162–1169.

[17] P.G. Mullins, H. Chen, J. Xu, A. Caprihan, C. Gasparovic, Comparative reliability of proton spectroscopy techniques designed to improve detection of J-coupled metabolites, Magn. Reson. Med. 60 (4) (2008) 964–969.

[18] J.A. Pople, W.G. Schneider, H.J. Bernstein, High-Resolution Nuclear Magnetic Resonance, McGraw-Hill, New York, 1959.

[19] V. Govindaraju, K. Young, A.A. Maudsley, Proton NMR chemical shifts and coupling constants for brain metabolites, NMR Biomed. 13 (3) (2000) 129–153.

[20] A.H. Trabesinger, D. Meier, U. Dydak, R. Lamerichs, P. Boesiger, Optimizing PRESS localized citrate detection at 3 Tesla, Magn. Reson. Med. 54 (1) (2005) 51–58.

[21] A.A. Maudsley, V. Govindaraju, K. Young, Z.K. Aygula, P.M. Pattany, B.J. Soher, G.B. Matson, Numerical simulation of PRESS localized MR spectroscopy, J. Magn. Reson. 173 (1) (2005) 54–63.

[22] H. Kim, R.B. Thompson, C.C. Hanstock, P.S. Allen, Variability of metabolite yield using STEAM or PRESS sequences in vivo at 3.0 T, illustrated with myo-inositol, Magn. Reson. Med. 53 (4) (2005) 760–769.

[23] J. Snyder, R.B. Thompson, J.M. Wild, A.H. Wilman, Strongly coupled versus uncoupled spin response to radio frequency interference effects: application to glutamate and glutamine in spectroscopic imaging, NMR Biomed. 21 (4) (2008) 402–409.

[24] R.B. Thompson, P.S. Allen, Response of metabolites with coupled spins to the STEAM sequence, Magn. Reson. Med. 45 (6) (2001) 955–965.

[25] R.B. Thompson, P.S. Allen, The role of the N-acetylaspartate multiplet in the quantification of brain metabolites, Biochem. Cell Biol.: Biochim. Biol. Cell. 76 (2–3) (1998) 497–502.

[26] A. Yahya, P.S. Allen, Effect of strong homonuclear proton coupling on localized C-13 detection using PRESS, Magn. Reson. Med. 54 (6) (2005) 1340–1350.

[27] J. Snyder, C.C. Hanstock, A.H. Wilman, Spectral editing of weakly coupled spins using variable flip angles in PRESS constant echo time difference spectroscopy: application to GABA. J. Magn. Reson. 200 (2) (2009) 245–250.

[28] P.J.W. Pouwels, K. Brockmann, B. Kruse, B. Wilken, M. Wick, F. Hanefeld, J. Frahm, Regional age dependence of human brain metabolites from infancy to adulthood as detected by quantitative localized proton MRS, Pediatr. Res. 46 (4) (1999) 474–485.

[29] S.W. Provencher, Estimation of metabolite concentrations from localized in vivo proton NMR spectra, Magn. Reson. Med. 30 (6) (1993) 672–679.
[30] K.L. Behar, D.L. Rothman, D.D. Spencer, O.A.C. Petroff, Analysis of macromolecule resonances in 1H NMR spectra of human brain, Magn. Reson. Med. 32 (3) (1994) 294–302.
[31] C.H. Choi, P.P. Bhardwaj, S. Kalra, C.A. Casault, U.S. Yasmin, P.S. Allen, N.J. Coupland, Measurement of GABA and contaminants in gray and white matter in human brain in vivo, Magn. Reson. Med. 58 (1) (2007) 27–33.